© 2018. Published by The Company of Biologists Ltd | Journal of Cell Science (2018) 131, jcs216671. doi:10.1242/jcs.216671

RESEARCH ARTICLE

p38δ MAPK regulates aggresome biogenesis by phosphorylating SQSTM1 in response to proteasomal stress

Chenliang Zhang[1,2,3], Ju Gao[1,2], Mengen Li[1,2], Yongkang Deng[1,2] and Changan Jiang[1,2,3,*,‡]

ABSTRACT

Aggresome formation is a major strategy to enable cells to cope with proteasomal stress. Misfolded proteins are assembled into micro-aggregates and transported to the microtubule organizing center (MTOC) to form perinuclear aggresomes before their degradation through autophagy. So far, multiple factors have been identified as the activators of micro-aggregate formation, but much less is known about the regulatory mechanisms of their transport. Here, we report that proteasomal stress leads to the activation of p38 MAPK family members. Two of them, p38γ (MAPK12) and p38δ (MAPK13), are dispensable for micro-aggregate formation but are required for their targeting to the MTOC. Interestingly, p38δ promotes micro-aggregate transport by phosphorylating SQSTM1, a major scaffold protein that assembles soluble ubiquitylated proteins into micro-aggregates. Expression of the phospho-mimetic mutant of SQSTM1 in p38δ-knockout cells completely rescued their aggresome formation defects and enhanced their resistance to proteasomal stress to wild-type levels. This study reveals p38δ-mediated SQSTM1 phosphorylation as a critical signal for the targeting of micro-aggregates to the MTOC and provides direct evidence for the survival advantages associated with aggresome formation in cells under proteasomal stress.

KEY WORDS: Aggresome, Autophagy, p38, Proteasome inhibition, SQSTM1

INTRODUCTION

Aggresome formation is an important strategy that many cell types employ to reduce the proteotoxic stress associated with insufficient proteasome activity. Through active transport of misfolded proteins to centralized depositories, cells can prevent these dysfunctional molecules from sequestering critical factors and facilitate their degradation through autophagy (Fortun et al., 2003; Johnston et al., 1998). Studies on cultured cells treated with proteasome inhibitors revealed that aggresome formation consists of two steps. First, misfolded proteins, often polyubiquitylated, are assembled into micro-aggregates in the cytosol. Second, micro-aggregates are loaded onto dynein motors and transported along the microtubule network to the microtubule organizing center (MTOC), where they loosely congregate to form a large aggresome (Kawaguchi et al., 2003).

Significant progress has been made in our understanding of the packaging of ubiquitylated proteins into micro-aggregates during proteasome inhibition. At the center is a multi-domain protein SQSTM1 (Sequestesome 1, also known as p62), which serves as a scaffold for the assembly and activation of many signaling complexes, such as mTOR (mechanistic target of rapamycin serine/threonine kinase), TNFR (tumor necrosis factor receptor) and NOD2 (nucleotide binding oligomerization domain containing-2) (Durán et al., 2004; Linares et al., 2013; Park et al., 2013). SQSTM1 contains a Ub (ubiquitin)-associated domain (UbA domain) at its C-terminus, but under normal physiological conditions, it does not bind polyubiquitin chains because of steric hindrance (Bjørkøy et al., 2005; Lin et al., 2013). Proteasome inhibition stimulates its Ub-binding activity through the activation of three kinases, CK2 (casein kinase 2), ULK1 (unc-51 like autophagy activating kinase 1) and Pink1-s (short form of PTEN-induced putative kinase 1) (Gao et al., 2016; Lim et al., 2015; Matsumoto et al., 2011). After its phosphorylation, SQSTM1 binds the polyubiquitylated proteins and assembles them into micro-aggregates through self-oligomerization (Bjørkøy et al., 2005; Zatloukal et al., 2002).

Ub-binding proteins are also important for the transport of micro-aggregates to the MTOC, the second step in aggresome formation. A key player in this process is HDAC6 (histone deacetylase 6) (Kawaguchi et al., 2003). HDAC6 is a protein deacetylase with a dynein-binding domain and a Ub-binding BUZ domain (bound to the ubiquitin zinc finger domain). Unlike the UbA domain in SQSTM1, the BUZ domain only interacts with the diglycine motif at the C-termini of Ub monomers or unanchored Ub chains but not the polyubiquitin chains conjugated to the misfolded proteins. In the current model, after SQSTM1 assembles free-floating polyubiquitylated proteins into micro-aggregates scattered at the cell periphery, a polyubiquitin-editing enzyme AT3 (ataxin-3) is recruited to the micro-aggregates and generates unanchored Ub ends by cutting the middle of polyubiquitin chains (Ouyang et al., 2012). This allows the binding of HDAC6 to the surface of the micro-aggregates, which facilitates their loading onto the dynein motors and targeting to MTOC through microtubule network. Puzzlingly, perinuclear aggresome formation is a unique phenomenon associated with proteasomal inhibition. Many other stress agents, such as heavy metals and puromycin, can also cause the accumulation of misfolded proteins and formation of micro-aggregates in the cells, but they do not promote the formation of perinuclear aggresomes, suggesting that there must be a proteasomal stress-activated signaling pathway that controls the transport of micro-aggregates to the MTOC (Szeto et al., 2006; Travassos et al., 2017).

p38 mitogen-activated protein kinases (MAPKs) form a family of evolutionary conserved protein kinases that can be activated by many growth factors, cytokines and environmental stresses. It consists of four members, p38α, p38β, p38γ and p38δ

[1]Department of Pediatrics, West China 2nd University Hospital, Sichuan University, Chengdu, Sichuan 610041, China. [2]Key Laboratory of Obstetric, Gynecologic, Pediatric Diseases and Birth Defects, Ministry of Education, Sichuan University, Chengdu, Sichuan 610041, China. [3]State Key Laboratory of Biotherapy, Collaborative Innovation Center of Biotherapy, West China Hospital, Sichuan University, Chengdu, Sichuan 610041, China.
*Present address: Center of Precision Medicine, Zhuhai Institute of Advanced Technology, Chinese Academy of Sciences, Zhuhai, Guangdong 519080, China.

‡Author for correspondence (jiangorder@gmail.com)

C.Z., 0000-0003-2274-2657; J.G., 0000-0001-5893-9406; M.L., 0000-0003-0102-9289; Y.D., 0000-0001-5723-0542; C.J., 0000-0002-1612-2470

Received 8 February 2018; Accepted 8 June 2018

Journal of Cell Science (2018) 131, jcs216671. doi:10.1242/jcs.216671

(MAPK14, MAPK11, MAPK12 and MAPK13, respectively) (Coulthard et al., 2009; Cuadrado and Nebreda, 2010). Multiple studies have indicated that there is cross-talk between SQSTM1 and p38 MAPKs leading to the activation of different signaling pathways. For example, SQSTM1 is required for the activation of p38α in response to cytokine stimulation and UV irradiation (Kawai et al., 2008). Conversely, phosphorylation of SQSTM1 by p38δ is required for the activation of the mTOR complex 1 in response to amino acid stimulation (Linares et al., 2013). Given the central roles that SQSTM1 plays during aggresome formation, these results raise the possibility that p38 MAPKs also regulate this process.

In this report, we show that proteasome inhibition activates all four p38 MAPK family members. While p38α and p38β are dispensable for aggresome formation, p38γ and p38δ are required for the efficient transport of micro-aggregates to the MTOC. Loss of p38γ or p38δ led to the failure of aggresome formation and the accumulation of scattered micro-aggregates in the cytosol. A more detailed analysis of p38δ revealed that it interacts with SQSTM1 in a proteasomal stress-dependent manner and promotes aggresome biogenesis by phosphorylating SQSTM1 at Thr269 and Ser272 residues. These results suggest that proteasomal stress not only directs the assembly of misfolded proteins into micro-aggregates, but also directs the recruitment of micro-aggregates to perinuclear aggresomes for autophagic degradation.

RESULTS

p38γ and p38δ MAPKs are activated by proteasome inhibition and are required for aggresome formation

To uncover the potential functions of p38 MAPKs in the proteasomal stress response, we first examined whether they could be activated in cells treated with proteasome inhibitors. Activation of p38 MAPKs requires dual phosphorylation at the Thr-Gly-Tyr motif (TGY motif) in their activation loops, which can be quantified by western blot analysis with a TGY motif phosphorylation antibody, such as the phospho-p38(T180/Y182) antibody (Coulthard et al., 2009; Cuadrado and Nebreda, 2010). Each p38 family member was tagged with FLAG and expressed in AD293 cells by transient transfection. The cells were next treated with 2 µM MG132 for 12 h and the phosphorylation of FLAG-p38 was analyzed by western blot analysis. As shown in Fig. 1A,B, MG132 treatment induced phosphorylation in all p38 MAPKs. To exclude the possibility that MG132 might activate p38 MAPKs by causing other unintended types of stress, we used another proteasome inhibitor, Bortezomib, to treat the cells. Bortezomib also induced the phosphorylation of all overexpressed p38 family members, suggesting that proteasomal stress is a physiological signal for the activation of p38 MAPK pathways (Fig. S1A).

Western blot analysis indicated that all four members of p38 MAPKs are expressed in AD293 cells (Fig. 1C). To determine their phosphorylation status during proteasomal stress, we analyzed the lysates of MG132-treated AD293 cells by western blot analysis with the same antibody used above to detect phosphorylation. In control cells, the levels of p38 phosphorylation are low, but after MG132 treatment, three distinct bands could be detected by western blot analysis (Fig. 1C). To determine the identity of each band unequivocally, we used CRISPR/Cas9 to generate knockout cell lines for each p38 family member from AD293 cells (Cong et al., 2013; Mali et al., 2013). Western blot analysis verified the complete loss of the target gene expression in these cell lines (Fig. S1B). A comparison of the p38 phosphorylation patterns in the mutant cells with that in WT cells indicated that MG132 induced robust phosphorylation of endogenous p38γ and p38δ (Fig. 1C). Phosphorylated p38α and p38β had similar mobility on the blot, so it is difficult to determine their respective phosphorylation levels in the WT cells. However, western blot results of p38α$^{-/-}$ and p38β$^{-/-}$ cells showed that the band corresponding to the phosphorylated p38α/β was induced in both knockout cell lines after MG132 treatment, suggesting that both of them could be activated by proteasome inhibition as well (Fig. 1C).

To test whether any of the p38 family members are required for aggresome formation, we treated the knockout cell lines with MG132 and analyzed the distribution of ubiquitylated proteins by immunostaining the cells with Ub(K48) antibody, which specifically recognizes the K48-linked polyubiquitin chain. Perinuclear aggresomes were detected in 72.9% of the WT cells. In p38α$^{-/-}$ and p38β$^{-/-}$ cells, aggresome formation rates were 68.7% and 66.8%, respectively, which represented a small but non-significant reduction from levels in the WT cells. In contrast, aggresome formation rates in p38γ$^{-/-}$ and p38δ$^{-/-}$ cells were 15.3% and 11.2%, respectively, which represented a 79.0% and 84.6% reduction compared with WT cells. Instead of forming perinuclear aggresomes, ubiquitylated proteins in most p38γ$^{-/-}$ and p38δ$^{-/-}$ cells formed micro-aggregates scattered throughout the cytosol (Fig. 1D,E). Re-expression of exogenous p38γ or p38δ in their corresponding knockout cells effectively suppressed their aggresome formation defects (Fig. S1C-E,F-H). These results suggested that p38γ and p38δ, but not p38α or p38β, are required for aggresome formation during proteasomal stress. More importantly, the accumulation of micro-aggregates in p38γ$^{-/-}$ and p38δ$^{-/-}$ cells after MG132 treatment implicates these two p38 family members as essential regulatory factors for the transport of micro-aggregates to the MTOC.

p38δ localizes to the aggresomes

As a first step to determine the molecular mechanisms underlying the aggresome-promoting activities of p38γ and p38δ, we examined their subcellular localizations during proteasomal stress. AD293 cells were transfected with one of the plasmids expressing aggresome markers, FLAG-Ub, FLAG-SQSTM1 or FLAG-HDAC6, and treated with MG132. Immunofluorescence staining showed strong co-localization of the endogenous p38δ with overexpressed Ub, SQSTM1 and HDAC6 in the perinuclear aggresomes, indicating that p38δ is targeted to the aggresomes during proteasomal stress (Fig. 2A). Consistent with this result, FLAG-p38δ overexpressed in p38δ$^{-/-}$ cells was also exclusively localized in the aggresomes during proteasomal stress (Fig. S1G). In contrast, although overexpressed FLAG-p38γ rescued the aggresome formation defect of p38γ$^{-/-}$ cells, it did not show strong localization in the aggresomes during proteasome inhibition, suggesting that it promotes aggresome formation through a different mechanism (Fig. S1D).

Since proteins in the aggresome cannot be solubilized by mild detergent, such as 1% Triton X-100 or NP40, it is possible to analyze the localization of endogenous p38 MAPKs biochemically (Gao et al., 2016). In cells under normal physiological conditions, virtually all p38 family members were localized in the NP40-soluble fraction, but in MG132-treated cells, p38δ, but not p38β or p38γ, could be readily detected in the NP40-insoluble fraction (Fig. 2B,C). This change in distribution of p38δ is similar to that of the aggresome marker SQSTM1, suggesting that it is an intrinsic component of micro-aggregates/aggresomes formed during proteasomal stress. Interestingly, low levels of p38α were also detected in the NP40-insoluble fraction of MG132-treated cells, suggesting that proteasome inhibition triggers its translocation into micro-aggregates/aggresomes as well. However, since p38α$^{-/-}$ cells do not display any aggresome

Journal of Cell Science (2018) 131, jcs216671. doi:10.1242/jcs.216671

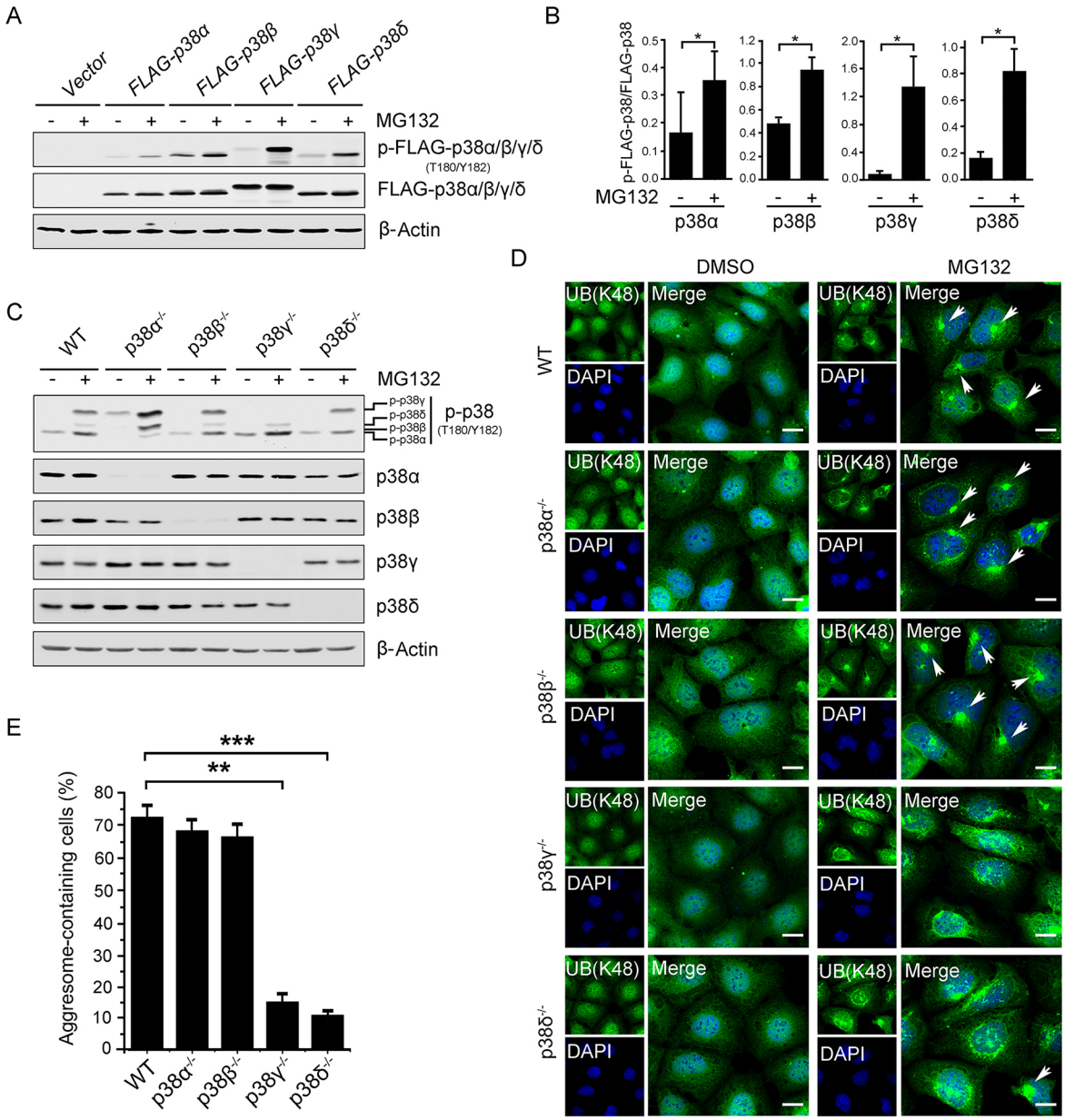

Fig. 1. p38γ and p38δ are activated by proteasome inhibition and are required for aggresome formation. (A) MG132 treatment induces the phosphorylation in the activation loops of p38 MAPKs transiently expressed in AD293 cells. AD293 cells were transfected with FLAG-p38α, FLAG-p38β, FLAG-p38γ or FLAG-p38δ expression plasmid and treated with DMSO (control) or 2 µM MG132 for 12 h. p38 expression and activation was detected by western blot analysis with FLAG and phospho-p38(T180/Y182) antibody, respectively. β-actin was detected as a loading control. (B) Quantitative analysis of p38(T180/Y182) phosphorylation results in A. Data are mean±s.e.m. of three independent experiments; **P*<0.05. (C) MG132 treatment induces the activation of the endogenous p38 MAPKs in AD293 cells. Wild-type (WT), p38α$^{-/-}$, p38β$^{-/-}$, p38γ$^{-/-}$ and p38δ$^{-/-}$ AD293 cells were treated with DMSO or 2 µM MG132 for 12 h. Whole cell lysates were subjected to SDS-PAGE and western blot analysis with indicated antibodies. β-actin was detected as a loading control. (D) Aggresome formation in WT, p38α$^{-/-}$, p38β$^{-/-}$, p38γ$^{-/-}$ and p38δ$^{-/-}$ cells after treated with DMSO or 2 µM MG132 for 14 h. Micro-aggregates and aggresomes were detected by immunostaining with Ub(K48) (green) antibody and the nuclei were detected by DAPI staining (blue). Ub(K48)-containing aggresomes are indicated with arrowheads. Scale bars: 20 µm. (E) Quantitative analysis of aggresome formation efficiency in MG132-treated cells treated as in D. For each experiment, 50 cells were randomly selected from each cell line to score for aggresomes. Data are shown as mean±s.e.m. of three independent experiments. ***P*<0.01; ****P*<0.001.

formation defect, most likely the translocation of p38α is not related to the activation of aggresome biogenesis.

Our previous study indicated that ubiquitylated proteins in HeLa cells rarely form aggresomes when treated with proteasome inhibitors. They form micro-aggregates in the cytosol. This phenotype is similar to the aggresome formation defect we observed in p38γ$^{-/-}$ and p38δ$^{-/-}$ cells. To determine whether the accumulation of micro-aggregates is related to p38 MAPKs, we examined the expression levels of p38 members in HeLa cells by western blot analysis. Compared with AD293 cells, HeLa cells expressed slightly reduced levels of p38α, p38β and p38γ, but much lower levels of p38δ (Fig. 2D,E). This raises a possibility that the aggresome formation defect in HeLa cells is due to their lack of p38δ expression. To test this hypothesis, we generated HeLa cell lines stably overexpressing FLAG-p38δ. Under proteasome inhibition, 75.1% of the HeLa(FLAG-p38δ) cells formed an aggresome, an efficiency comparable to that of AD293

Journal of Cell Science (2018) 131, jcs216671. doi:10.1242/jcs.216671

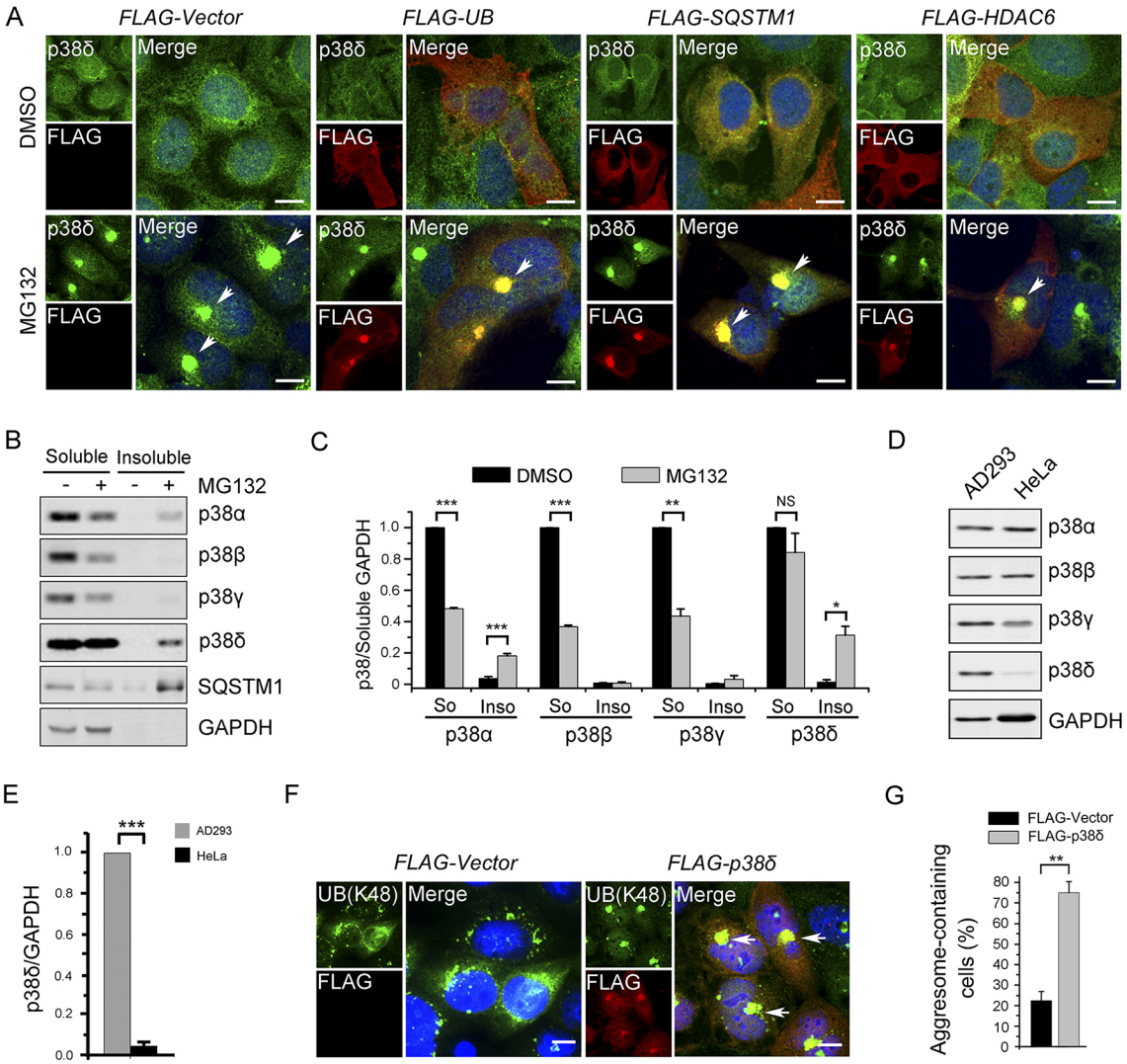

Fig. 2. p38δ is targeted to aggresomes during proteasome inhibition. (A) Co-localization of p38δ with aggresome makers Ub, SQSTM1 and HDAC6 during proteasome inhibition. AD293 cells were transfected with control plasmid (FLAG vector) or plasmid expressing aggresome maker FLAG-Ub, FLAG-SQSTM1 or FLAG-HDAC6. After 24 h, cells were treated with DMSO or 2 µM MG132 for 14 h, and immunostained with p38δ (green) and FLAG (red) antibodies. Nuclei are stained with DAPI (blue). Aggresomes are indicated with arrowheads. Scale bars: 10 µm. (B) Western blot analysis of p38 MAPKs in NP40-soluble and -insoluble protein fractions of AD293 cells after proteasome inhibition. AD293 cells were treated with DMSO or 2 µM MG132 for 12 h, and lysed with 1% NP40 lysis buffer. For each sample, 5% of the soluble fraction and 20% of the insoluble fraction were subjected to western blot analysis with indicated antibodies. Soluble GAPDH was detected and used as a loading control. (C) Quantitative analysis of results in B. So, soluble fraction; Inso, insoluble fraction. (D) Whole-cell lysates of AD293 and HeLa cells were subjected to SDS-PAGE and western blot analysis with indicated antibodies. GAPDH is detected as a loading control. (E) Quantitative analysis of p38δ expression in D. (F) Proteasome inhibition induced aggresome formation in p38δ-expressing HeLa cells. HeLa cells stably expressing FLAG-vector or FLAG-p38δ were treated with 2 µM MG132 for 14 h, and immunostained with Ub(K48) antibody (green) and FLAG antibody (red). The nuclei were stained with DAPI (blue). Ub(K48)-containing aggresomes are indicated with arrowheads. Scale bar: 15 µm. (G) Quantitative analysis of results shown in F. For each experiment, 50 cells were randomly selected from each cell line to score for aggresomes. All data are mean±s.e.m. of three independent experiments. *P<0.05; **P<0.01; ***P<0.001.

cells (Fig. 2F,G). Immunofluorescence staining indicated that FLAG-p38δ is also localized in the aggresome in HeLa(FLAG-p38δ) cells (Fig. 2F). These results argue that p38δ is a common regulator required for the targeting of micro-aggregates to the MTOC in different cell types, so we decided to focus our mechanistic study on p38δ.

Proteasome inhibition promotes the interaction between p38δ and SQSTM1

The co-localization of p38δ and SQSTM1 in aggresomes raises a possibility that p38δ may promote aggresome formation through SQSTM1. A p38δ-SQSTM1 link has been reported before. During amino acid-induced mTOR complex 1 activation, p38δ and its upstream kinases, MEK3/6 and MEKK3, form a signaling complex with SQSTM1 (Linares et al., 2013). Phosphorylation of SQSTM1 by p38δ promotes the recruitment of TRAF6 (TNF receptor associated factor 6), an Ub E3 ligase, to the mTORC1 complex. This leads to the ubiquitylation of mTOR and full activation of mTORC1. To test whether p38δ and SQSTM1 have a similar regulatory relationship during proteasomal stress, we first examined their interaction during proteasome inhibition by immunoprecipitation. AD293 cells were co-transfected with FLAG-SQSTM1 and MYC-p38δ plasmids. After MG132 treatment, anti-FLAG antibody was used to pull down FLAG-SQSTM1 and its

Journal of Cell Science (2018) 131, jcs216671. doi:10.1242/jcs.216671

associated proteins. Western blot analysis showed that in control cells, only a small amount of MYC-p38δ could be pulled down by FLAG-SQSTM1, but in cells treated with MG132, the levels of MYC-p38δ pulled down significantly increased, suggesting that proteasomal stress promoted the association of SQSTM1 and p38δ (Fig. 3A). We also examined binding of endogenous SQSTM1 and p38δ by immunoprecipitating with anti-SQSTM1 antibody and found that their interaction was negligible in control cells, but dramatically increased in cells treated with MG132 (Fig. 3B). Although the use of immunoprecipitation here limited our assay of any protein interaction in the NP40-soluble fraction, the dramatic increase of p38δ-SQSTM1 association we observed here argues that the free-floating p38δ and SQSTM1 form a complex before they are assembled into micro-aggregates/aggresomes during proteasomal stress.

Since SQSTM1 is a substrate of p38δ, it is likely that proteasome inhibition promotes p38δ-SQSTM1 interaction simply by activating p38δ and allowing it to bind its substrate. We tested this hypothesis by examining whether the binding of p38δ to SQSTM1 was dependent on its kinase activity using a kinase-dead mutant of p38δ, p38δ(K54R), and a constitutively active mutant, p38δ(F324S) (Askari et al., 2007; Koul et al., 2013). In cells treated with MG132, both MYC-p38δ(K54R) and MYC-p38δ(F324S) pulled down FLAG-SQSTM1 as efficiently as their WT counterpart did, suggesting that p38δ-SQSTM1 interaction was not dependent on the proteasome inhibition-triggered activation of p38δ (Fig. 3C). Consistent with the biochemical result, both p38δ(K54R) and p38δ(F324S) were efficiently targeted to aggresomes in MG132-treated cells (Fig. S2). Given that SQSTM1 undergoes a dramatic conformational change during proteasomal stress, it is likely to be responsible for recruitment of p38δ to the micro-aggregates and aggresomes.

SQSTM1 has seven identified domains that mediate its interaction with other proteins (Fig. 3D) (Lin et al., 2013). We sought to map out the area important for its interaction with p38δ. To eliminate the interference of endogenous SQSTM1, we carried out this experiment in a SQSTM1-knockout cell line we generated earlier. AD293(SQSTM1$^{-/-}$) cells were transfected with plasmids expressing MYC-p38δ along with FLAG-tagged full-length SQSTM1 or one of its four deletion mutants, F1, F2, F3 or F4. After MG132 treatment, cells were lysed and subjected to immunoprecipitation with anti-FLAG antibody. In addition to the full-length SQSTM1, MYC-p38δ could be pulled down by the

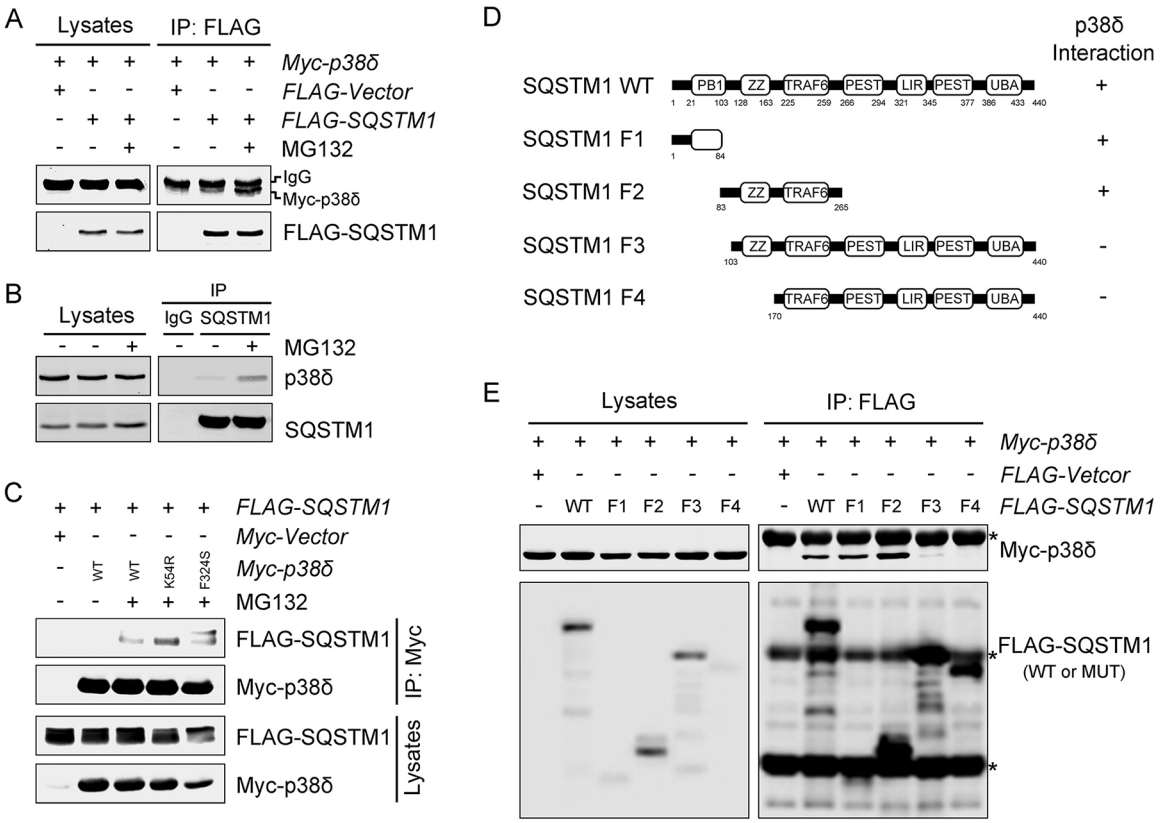

Fig. 3. Proteasome inhibition induces the association of p38δ with SQSTM1. (A) MG132 treatment induces the association of p38δ with SQSTM1 overexpressed in AD293 cells. AD293 cells were transfected with indicated plasmids. After 24 h, cells were treated with DMSO or 1 µM MG132 for 12 h. FLAG-SQSTM1 was immunoprecipitated with FLAG antibody from the cell lysates, and the associated MYC-p38δ was detected with MYC antibody. (B) MG132 treatment induces the association of endogenous p38δ with SQSTM1 in AD293 cells. AD293 cells were treated with DMSO or 1 µM MG132 for 12 h, lysed and immunoprecipitated with control IgG or SQSTM1 antibody. The associated p38δ was detected by western blot analysis. (C) MG132-induced p38δ binding to SQSTM1 was not dependent on its kinase activity. AD293 cells were transfected with indicated plasmids. After 24 h, cells were treated with DMSO or 1 µM MG132 for 12 h. MYC-p38δ was immunoprecipitated from the cell lysates with MYC antibody and the associated FLAG-SQSTM1 was detected by western blot analysis with FLAG antibody. (D) Structure of WT SQSTM1 and its deletion mutants used for the mapping of p38δ-interacting domain. PB1, Phox and Bem 1 domain; ZZ, zinc finger motif domain; TRAF6, TRAF6-interacting domain; PEST, amino acids Pro, Glu, Ser, Thr-enriched domain; LIR, LC3-interacting region; UBA, Ub-associated domain. (E) Immunoprecipitation analysis of p38δ with the WT SQSTM1 and its deletion mutants. AD293(SQSTM1$^{-/-}$) cells were transfected with indicated plasmids. Cells were treated with 1 µM MG132 for 12 h after 24 h of expression. The FLAG-tagged WT and mutant SQSTM1 were immuoprecipitated from the cell lysate with FLAG antibody, and the associated MYC-p38δ was detected by western blot analysis with MYC antibody. Asterisks indicate IgG.

Journal of Cell Science (2018) 131, jcs216671. doi:10.1242/jcs.216671

F1 fragment, which contains the PB1 domain, and F2 fragment, which contains the ZZ and TRAF6-interaction domain, suggesting that P38δ binds to the N-terminus of SQSTM1 (Fig. 3E).

p38δ phosphorylates SQSTM1 at Thr269/Ser272 residues during proteasome inhibition

The activation of p38δ and its association with SQSTM1 in cells under proteasome inhibition strongly suggests that p38δ regulates aggresome formation through the phosphorylation of SQSTM1. During amino acid-induced activation of mTORC1, p38δ phosphorylates Thr269 and Ser272 residues in SQSTM1 (Linares et al., 2013). To examine whether the p38δ phosphorylates the same residues during proteasomal stress, we co-expressed FLAG-SQSTM1 and FLAG-p38δ in AD293 cells and measured the phosphorylation of SQSTM1 by western blot analysis with an anti-phospho-SQSTM1(T269/S272) antibody. Phosphorylation of FLAG-SQSTM1 was detected in cells with normal proteasome activities, but significantly higher levels of phosphorylation were detected in cells treated with MG132 (Fig. 4A). A similar result was obtained in HeLa cells (Fig. S3A). In another experiment,

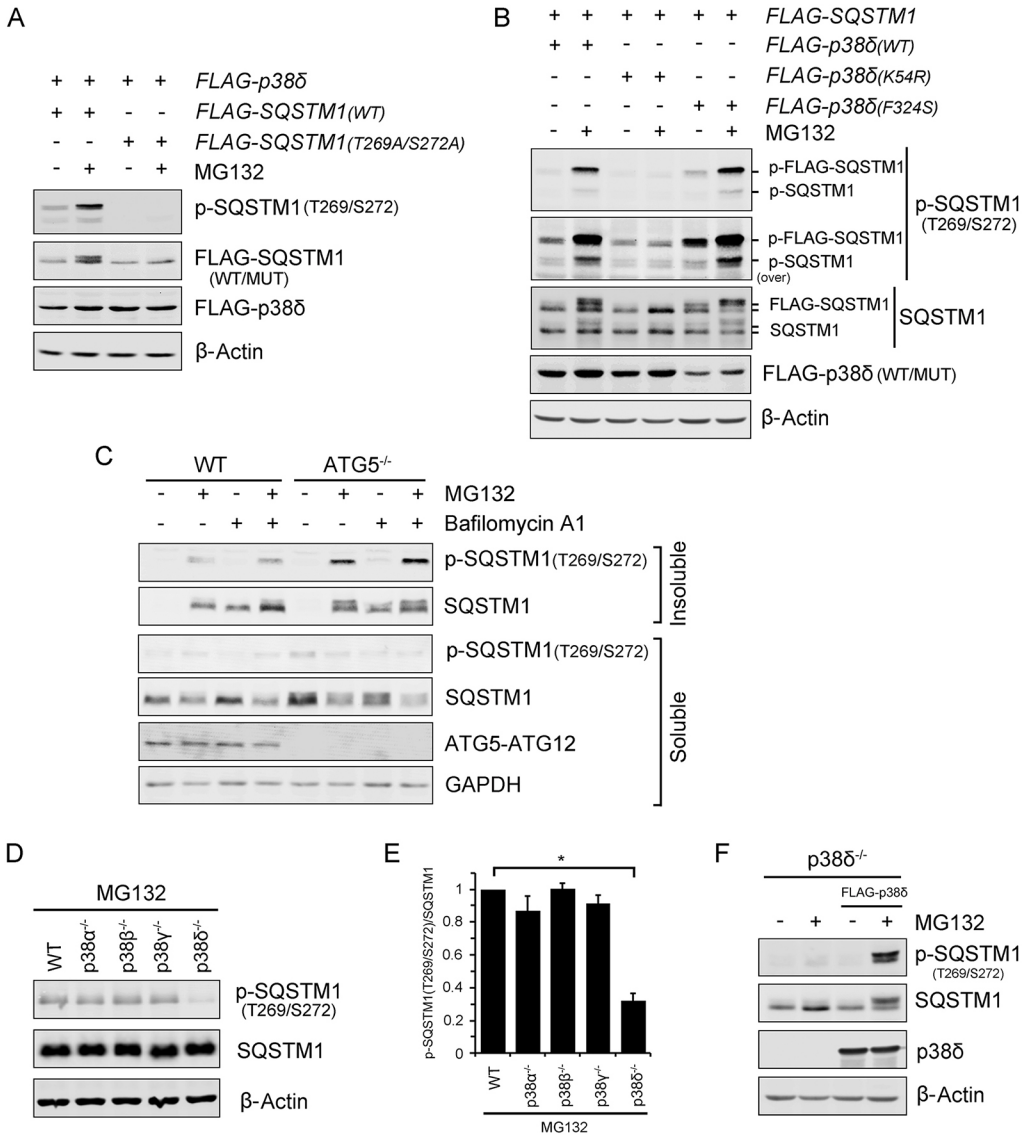

Fig. 4. Proteasome inhibition-activated p38δ phosphorylates SQSTM1. (A) p38δ phosphorylates Thr269/Ser272 residues of SQSTM1 during proteasome inhibition. AD293 cells were transfected with the indicated plasmids. After 24 h, cells were treated with DMSO or 1 μM MG132 for 12 h. Phosphorylation of Thr269/Ser272 in SQSTM1 was detected by western blot analysis with phospho-SQSTM1(T269/S272) antibody. The overexpressed p38δ and SQSTM1 were detected with FLAG antibody. β-actin was detected as a loading control. (B) Proteasome inhibition stimulates the phosphorylation of SQSTM1 by the constitutively active p38δ(F324S). AD293 cells were transfected with indicated plasmids, treated with MG132 and analyzed by western blotting as described in A. Over, overexposure. (C) Inhibition of autophagasome formation increases the levels of SQSTM1 with Thr269/Ser272 phosphorylation. WT and ATG5$^{-/-}$ AD293 cells were treated with DMSO, MG132 (1 μM) or MG132 (1 μM)/Bafilomycin A1 (100 nM) for 12 h. The cells were lysed with 1% NP40 lysis buffer. For each sample, 5% of the soluble fractions and 20% of the insoluble fractions were subjected to western blot analysis. Soluble GAPDH was detected and used as loading control. (D) Western blot analysis of SQSTM1 Thr269/Ser272 phosphorylation in the NP40-insoluble fractions of the WT, p38α$^{-/-}$, p38β$^{-/-}$, p38γ$^{-/-}$ and p38δ$^{-/-}$ AD293 cells after MG132 treatment. Cells were treated with 2 μM MG132 for 12 h and lysed with 1% NP40 lysis buffer. The insoluble fractions were subjected to western blot analysis with the indicated antibodies. (E) Quantitative analysis of results in D. Data are mean±s.e.m. of three independent results. *P<0.05. (F) Western blot analysis of SQSTM1 Thr269/Ser272 phosphorylation in p38δ$^{-/-}$ and its rescue cell line. p38δ$^{-/-}$ and p38δ$^{-/-}$(FLAG-p38δ) cells were treated with DMSO or 1 μM MG132 for 12 h. Whole cell lysates were subjected to western blot analysis with indicated antibodies.

Journal of Cell Science (2018) 131, jcs216671. doi:10.1242/jcs.216671

co-expression of the kinase-dead mutant of p38δ, p38δ(K54R), did not induce SQSTM1 phosphorylation even after MG132 treatment (Fig. 4B). Interestingly, co-expression of the constitutively active p38δ(F324S) only marginally increased SQSTM1 phosphorylation in the absence of proteasome inhibitors, and the phosphorylation levels increased markedly after MG132 treatment (Fig. 4B). This result suggests that proteasomal stress-induced recruitment of p38δ to SQSTM1 is required for the efficient phosphorylation of SQSTM1 at Thr269/Ser272.

We tried to detect Thr269/Ser272 phosphorylation of the endogenous SQSTM1 from the lysates of MG132-treated cells, but the results were not always consistent. We reasoned that this could be due to the localization of the phosphorylated SQSTM1 in the NP40-insoluble protein aggregates/aggresomes during proteasome inhibition. Western blot analysis of the NP40-insoluble fraction confirmed this possibility. In control cells, SQSTM1 was only detected in the soluble fraction, but in cells treated with MG132, SQSTM1 accumulated in the NP40-insoluble fraction and its phosphorylation at Thr269/Ser272 was readily detectable with the phosphorylation antibody (Fig. 4C).

Because aggresomes are degraded through autophagy, we decided to examine the effects of autophagy inhibition on the levels of phosphorylated SQSTM1. We first used a ATG5 knockout cell line generated from AD293 that could not initiate autophagosome formation (Mizushima, 2007). As expected, the levels of phosphorylated SQSTM1 significantly increased in the NP40-insoluble fraction after the cells were treated with MG132 (Fig. 4C). Another way to inhibit autophagy is to use Bafilomycin A1, which blocks autophagosome-lysosome fusion. Addition of Bafilomycin A1 into MG132-treated cells significantly increased the levels of NP40-insoluble SQSTM1, but it only slightly increased the levels of phosphorylated SQSTM1 (Fig. 4C). The different effects of these two methods are surprising. However, since ATG5 knockout and Bafilomycin A1 treatment arrest autophagy at different stages, it is possible that the lack of effect in Bafilomycin A1-treated cells was caused by the de-phosphorylation of SQSTM1 during the early autophagy process.

To evaluate the contribution of p38δ to Thr269/Ser272 phosphorylation in SQSTM1 during proteasome inhibition, we examined the levels of phosphorylated SQSTM1 in the NP40-insoluble fractions of p38δ$^{-/-}$ and other p38 MAPK knockout cells. Compared with results in WT cells, loss of p38α, p38β or p38γ did not have a significant effect on MG132-induced SQSTM1 phosphorylation, but loss of p38δ reduced the level by 65% (Fig. 4D,E). Re-expression of FLAG-p38δ in p38δ$^{-/-}$ cells dramatically increased Thr269/Ser272 phosphorylation upon MG132 or Bortezomib treatment (Fig. 4F, Fig. S3B,C), suggesting that p38δ is the major kinase that mediates SQSTM1 phosphorylation at these two residues during proteasome inhibition.

Thr269/Ser272 phosphorylation of SQSTM1 promotes aggresome formation

We next examined whether phosphorylation of SQSTM1 at Thr269/Ser272 would promote aggresome formation. As the first step, we examined whether WT, non-phosphorylatable (T269A/S272A) or phosphomimetic (T269E/S272D) mutant of SQSTM1 could rescue the aggresome formation defect of SQSTM1$^{-/-}$ cells. We used a lentiviral system to generate SQSTM1$^{-/-}$ cells stably expressing different forms of SQSTM1 (Fig. S4A), and analyzed their aggresome formation by immunostaining with anti-Ub(K48) antibody. In response to MG132 treatment, 58.1% of cells expressing SQSTM1(WT) and 68.2% of the cells expressing SQSTM1(T269E/S272D) formed perinuclear aggresomes. In contrast, only 30.9% of cells expressing SQSTM1(T269A/S272A) formed aggresomes, suggesting that phosphorylation of SQSTM1 at Thr269/Ser272 is required for effective aggresome formation during proteasome inhibition (Fig. 5A,B).

If phosphorylation of Thr269/Ser272 residues in SQSTM1 mediates the aggresome-promoting effect of p38δ, then overexpression of the phosphomimetic mutant SQSTM1(T269E/S272D) in p38δ$^{-/-}$ cells should be able to rescue its aggresome formation defect. To test this, we expressed the WT and mutant SQSTM1 in p38δ$^{-/-}$ cells using a lentiviral system (Fig. S4B) and analyzed their aggresome formation efficiency during proteasome stress. In response to MG132 treatment, only 36.2% of the cells expressing SQSTM1(WT) and 29.1% of the cells expressing SQSTM1(T269A/S272A) formed aggresomes. Strikingly, 72.5% of the cells expressing SQSTM1(T269E/S272D) formed aggresomes (Fig. 5C,D), suggesting that phosphorylated SQSTM1 can effectively rescue the aggresome formation defect in p38δ$^{-/-}$ cells.

We also compared the aggresome-promoting effect of the WT and mutant SQSTM1 in HeLa cells. To facilitate the detection of aggresome formation, we co-expressed SQSTM1 with mRFP-tagged CFTRΔF508, a CFTR mutant normally degraded by proteasome (Sha et al., 2009). Proteasome inhibition causes accumulation of ubiquitylated proteins that are targeted to micro-aggregates or aggresomes, so they can serve as a fluorescent marker for micro-aggregates/aggresomes. In most of the cells expressing SQSTM1(WT) and SQSTM1(T269A/S272A), mRFP-CFTRΔF508 was localized in micro-aggregates after MG132 treatment, but in 69.4% of the cells expressing SQSTM1(T269E/S272D), it was localized in perinuclear aggresomes (Fig. 5E,F). These results strongly suggested that p38δ regulates aggresome formation mainly through phosphorylating Thr269/Ser272 residues in SQSTM1 during proteasome inhibition.

p38δ protects cells from proteasome inhibition-induced cell death by phosphorylating SQSTM1

Previous studies have demonstrated that aggresome formation protects against cell death caused by proteasome inhibition. To determine whether p38δ suppresses proteasomal stress-induced cell death, we analyzed the rates of apoptosis and necrosis in WT, p38δ$^{-/-}$ and its rescue cell line p38δ$^{-/-}$ (FLAG-p38δ) with annexin-V (ANXA5)-FITC and propidium iodide (PI) double staining after they were treated with MG132. As expected, loss of p38δ in AD293 cells significantly increased their vulnerability to proteasome inhibition. A 18 h treatment with 2 µM MG132 induced apoptosis (ANXA5^{+} PI^{-}) in 6.18% and necrosis (ANXA5^{-}PI^{+}) in 2.99% of the WT cells, whereas in p38δ$^{-/-}$ cells, the apoptosis and necrosis rates increased to 17.29% and 6.06%, respectively. Re-expression of FLAG-p38δ in p38δ$^{-/-}$ cells reduced the apoptosis and necrosis rate to 4.97% and 3.21%, respectively, thus restoring their resistance to proteasome inhibition to the WT levels (Fig. 6A,B). This result confirms that p38δ is required to protect cells against proteasome inhibition-induced apoptosis and necrosis.

To investigate whether the cytoprotective functions of p38δ is dependent on the phosphorylation of Thr269/Ser272 in SQSTM1, we also analyzed the MG132 sensitivity of p38δ$^{-/-}$ cells stably expressing SQSTM1(WT), SQSTM1(T269A/S272A) and SQSTM1(T269E/S272D). Compared with p38δ$^{-/-}$ cells, expression of SQSTM1(WT) or SQSTM1(T269A/S272A) did not increase its survival rate after MG132 treatment. In contrast,

Journal of Cell Science (2018) 131, jcs216671. doi:10.1242/jcs.216671

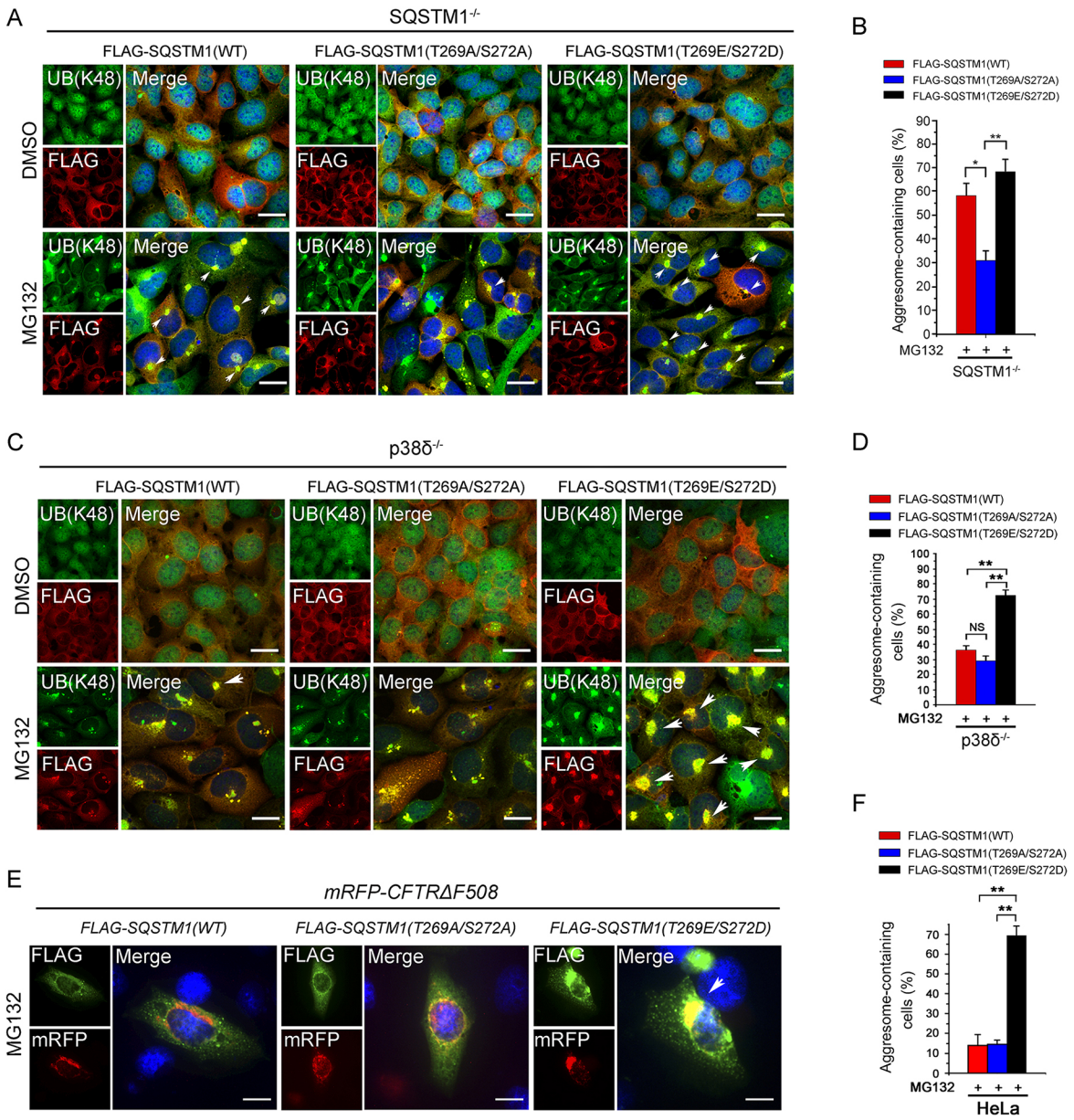

Fig. 5. Phosphomimetic SQSTM1 mutant rescues the aggresome formation defect in SQSTM1$^{-/-}$, p38δ$^{-/-}$ and HeLa cells. (A) Expression of SQSTM1(T269E/S272D) rescues the aggresome formation defect of SQSTM1$^{-/-}$ cells. SQSTM1$^{-/-}$ cells stably expressing WT or mutant SQSTM1 were treated with DMSO or 2 µM MG132 for 14 h and then immunostained with Ub(K48) (green) and FLAG (red) antibodies. The nuclei are stained with DAPI (blue). Aggresomes are indicated with arrowheads. Scale bars: 20 µm. (B) Quantitative analysis of results shown in A. (C) Expression of SQSTM1(T269E/S272D) rescued the aggresome formation defect of p38δ$^{-/-}$ cells. p38δ$^{-/-}$ cells stably expressing the WT and mutant FLAG-SQSTM1 were treated with DMSO or 2 µM MG132 for 14 h, then immunostained with Ub(K48) (green) and FLAG (red) antibodies. The nuclei were detected with DAPI staining (blue). Aggresomes are indicated with arrowheads. Scale bars: 20 µm. (D) Quantitative analysis of results shown in C. (E) HeLa cells were transfected with mRFP-CFTRΔF508 expression plasmid together with the WT or mutant FLAG-SQSTM1. After 24 h, cells were treated with 2 µM MG132 for 14 h and immunostained with FLAG antibody (green). The nuclei were detected by DAPI staining (blue). mRFP-CFTRΔF508-labelled aggresomes (red) are indicated with arrowheads. Scale bars: 10 µm. (F) Quantitative analysis of results shown in E. For B, D and E, 70 cells were randomly selected from each cell line to score for aggresomes. Data are mean±s.e.m. of three independent experiments. *P<0.05; **P<0.01; NS, not significant.

expression of SQSTM1(T269E/S272D) in p38δ$^{-/-}$ cells increased the survival rate from 62.23% to 77.71%. This was mainly achieved through a 64.5% reduction of apoptosis rate from 17.29% to 6.19% (Fig. 6C,D). A similar cytoprotective effect of SQSTM1(T269E/S272D) was observed in SQSTM1$^{-/-}$ cells (Fig. S4C,D). These results strongly suggest that recruitment of micro-aggregates to perinuclear aggresomes, a process activated by p38δ-mediated SQSTM1 phosphorylation, can protect cells by reducing their apoptosis rate during proteasomal stress.

DISCUSSION

Many types of stress, such as ER stress, oxidative stress and heavy metal exposure, can cause the accumulation of misfolded proteins, which tend to form small protein aggregates scattered in the cytosol (Hamdan et al., 2017; Tamás et al., 2014; Travassos et al., 2017). Among them, proteasomal stress is unique because it can further induce the transfer of micro-aggregates to the MTOC to form perinuclear aggresomes. This centralization process has been regarded as an adaptive response that can reduce the toxicity and

Journal of Cell Science (2018) 131, jcs216671. doi:10.1242/jcs.216671

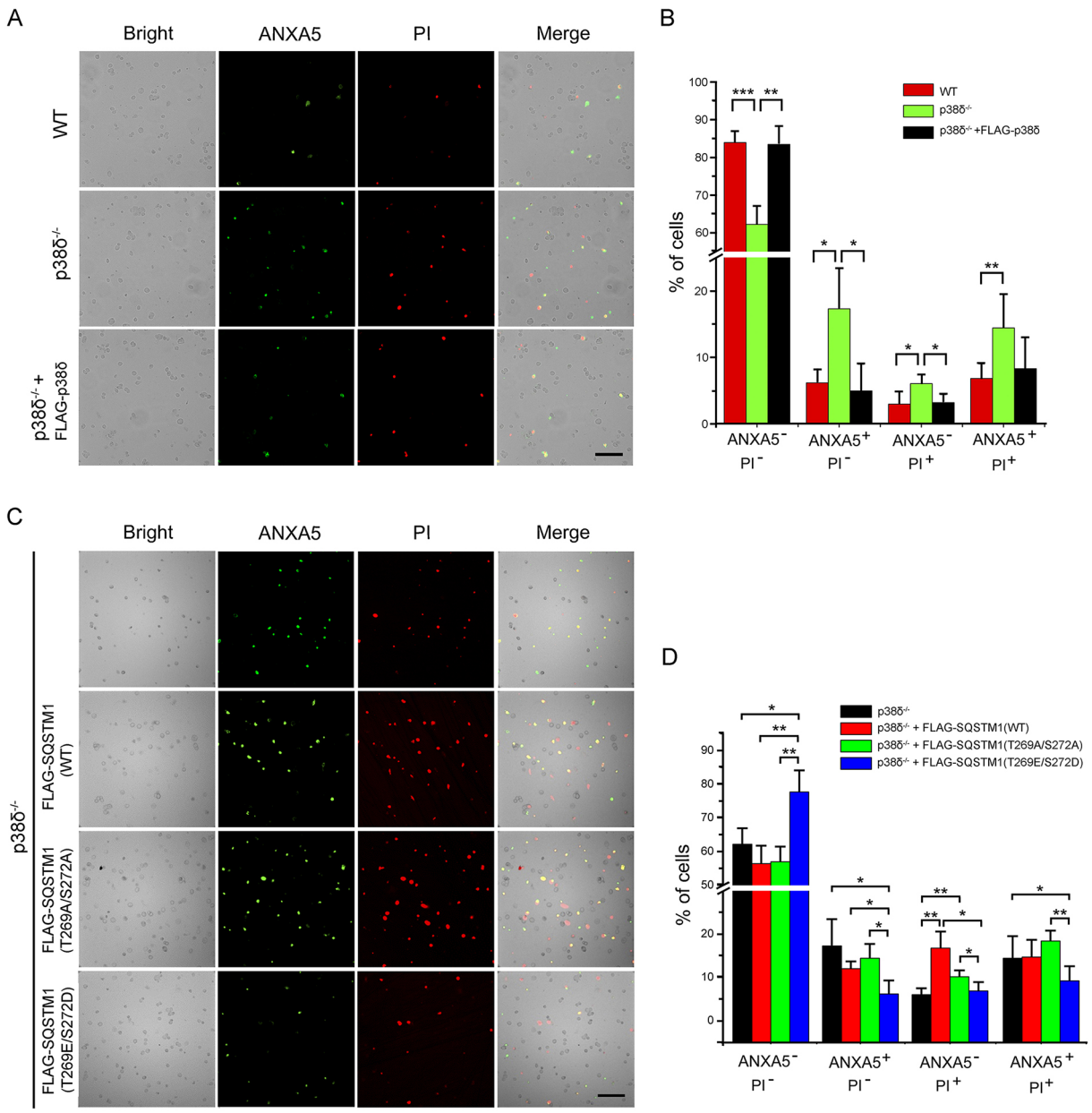

Fig. 6. Phosphomimetic SQSTM1 reduces proteasome inhibition-induced cell death. (A) Expression of exogenous P38δ reduces proteasome inhibition-induced P38δ$^{-/-}$ cell death. WT, p38δ$^{-/-}$ and p38δ$^{-/-}$(FLAG-p38δ) cells were treated with 2 µM MG132 for 18 h and stained with FITC-ANXA5 (Annexin V, green) and propidium iodide (PI, red) to detect dead cells. Live cells, ANXA5^{-}PI^{-}; early apoptotic cells, ANXA5^{+}PI^{-}; necrotic cells, ANXA5^{-}PI^{+}; late apoptotic cells, ANXA5^{+}PI^{+}. (B) Quantitative analysis of results in A. (C) Expression of phosphomimetic SQSTM1 reduced proteasome inhibition-induced p38δ$^{-/-}$ cell death. p38δ$^{-/-}$, p38δ$^{-/-}$(FLAG-SQSTM1), p38δ$^{-/-}$[FLAG-SQSTM1(T269A/S272A)] and p38δ$^{-/-}$[FLAG-SQSTM1(T269E/S272D)] cells were treated with MG132 and underwent cell death analysis as described in A. (D) Quantitative analysis of results in C. For B and D, 100 cells were randomly selected from each cell line to score for their ANXA5/PI signals. Data are shown as mean±s.e.m. of three independent experiments. *P<0.05; **P<0.01; ***P<0.001. Scale bars: 100 µm.

increase the degradation of misfolded proteins, but this hypothesis has not been carefully tested partly because the regulatory mechanisms controlling this process remain largely unclear (Johnston et al., 1998). In this study, we found that two p38 MAPKs, p38γ and p38δ, are activated by proteasome inhibition and required for the targeting of the micro-aggregates to the MTOC, a critical step in aggresome biogenesis (Fig. 1). These two p38 family members regulate aggresome formation via distinct mechanisms. While p38δ is recruited to SQSTM1 during proteasomal stress and promotes aggresome formation through phosphorylating SQSTM1 in the micro-aggregates/aggresomes, p38γ functions outside micro-aggregates/aggresomes and promotes aggresome formation through unknown mechanism(s). Therefore p38γ and p38δ control different signaling pathways that cooperate to promote the centralization of micro-aggregates during proteasomal stress.

It is a surprise that phosphorylation of Thr269/Ser272 in SQSTM1 is essential for the transport of the micro-aggregates. SQSTM1 is well known for its activity in the assembly of polyubiquitylated proteins into micro-aggregates and its function as an autophagy receptor to facilitate autophagosome formation around protein aggregates/aggresomes, the first step of their autophagic degradation (Gao et al., 2016; Lim et al., 2015; Matsumoto et al., 2011). Previous studies on micro-aggregate

transport have been focused on AT3 and HDAC6. In newly formed micro-aggregates, AT3 is responsible for the generation of unanchored polyubiquitin chains. This allows the recruitment of HDAC6, which loads the micro-aggregates onto dynein motors for microtubule transport (Kawaguchi et al., 2003; Ouyang et al., 2012). Although the model explains the retrograde direction of micro-aggregate transport, it does not provide a mechanism for its regulation by proteasomal stress. Our findings reported here partially fill this gap; however, they also raise a question about the relationship between p38δ-SQSTM1 and AT3-HDAC6. In a simple model, p38δ-mediated SQSTM1 phosphorylation may serve as a signal for the recruitment of AT3 to micro-aggregates or the activation of its deubiquitinase activity. Alternatively, phosphorylated SQSTM1 may be required for the activation of the protein deacetylase activity of HDAC6, which is also required for the transport of the micro-aggregates. Future study will address these possibilities.

Phosphorylation of SQSTM1 by p38δ was initially identified in amino acid-induced mTORC1 activation (Linares et al., 2013). SQSTM1 is the central scaffold molecule in the assembly of mTORC1 signaling hub. It is responsible for the recruitment of mTOR to the surface of lysosomes, a translocation event that is required for mTOR activation by RAG GTPases. p38δ is also required for the maximal activation of mTOR. Through its PB1 domain, SQSTM1 recruits MEKK3, the upstream kinase for MEK3/6 and p38δ, into an amino acid-sensing signaling complex. High levels of amino acid cause activation of the MEKK3-MEK3/6-p38δ kinase cascade, which phosphorylates SQSTM1 at Thr269/Ser272 residues. This leads to the recruitment of the Ub E3 ligase TRAF6 to the complex. It ubiquitylates mTOR and triggers its maximal activation. In this system, SQSTM1 brings p38δ to mTORC1 indirectly by interacting with MEKK3. In contrast, during proteasomal stress, SQSTM1 recruits p38δ to micro-aggregates directly, possibly through a conformational change that reveals its p38δ-binding sites at its N-terminus. Not surprisingly, our results also suggest that other components in the mTORC1 pathway do not participate in the regulation of micro-aggregate transport. In both MEKK3- and TRAF6-knockout cells, micro-aggregates can be efficiently transferred to the MTOC and form perinuclear aggresomes normally, suggesting that p38δ-SQSTM1 serves a generic signaling module that can mediate different physiological changes to activate corresponding downstream effectors (Fig. S5).

The identification of Thr269/Ser272 phosphorylation in SQSTM1 as a critical event in micro-aggregate transport allows us to precisely evaluate the functional significance of this process during proteasomal stress. So far, evidence to support the cytoprotective effects of this process mainly came from the observation that knockdown of AT3 or HDAC6 increases a cell's sensitivity toward MG132, but it is possible that such effects are due to other essential functions of these genes in unrelated signaling pathways (Kawaguchi et al., 2003; Ouyang et al., 2012). In this study, we examined the ability of WT, phosphomimetic and non-phosphorylatable mutants of SQSTM1 to rescue the death of p38δ$^{-/-}$ cells under proteasomal stress. Knockout of p38δ in AD293 cells dramatically reduces their aggresome formation efficiency and increases their sensitivity toward proteasome inhibitors. While expression of SQSTM1(WT) and nonphosphorylatable SQSTM1(T269A/S272A) in p38δ$^{-/-}$ cells only modestly increase their aggresome formation efficiency, expression of phosphomimetic SQSTM1(T269E/S272D) completely rescued their aggresome formation to wild-type levels. More strikingly, while SQSTM1(WT) and SQSTM1(T269A/S272A) did not provide significant protection for p38δ$^{-/-}$ cells under proteasomal stress, SQSTM1(T269E/S272D) reduced the apoptosis rate by 64.5% and increased the overall survival rate by 24.8% (Fig. 6C,D). This stark contrast provides a piece of strong evidence that transfer of micro-aggregates to perinuclear aggresomes effectively increases a cell's resistance to proteasome inhibition.

The direct activation of micro-aggregate transport by proteasomal stress is potentially important for the efficient autophagy of misfolded proteins. A few hours after proteasome inhibition, most ubiquitylated proteins and lysosomes inside the cells are concentrated around the MTOC, with the aggresome surrounded by lysosomes in each cell. This precise spatial arrangement presumably allows the systematic dismantling of the aggresome into smaller aggregates that undergo autophagy individually. Interestingly, lysosomes are enriched around the MTOC through a different mechanism during proteasome inhibition. A study by Zaarur et al. (2014) suggests that proteasome inhibition causes the formation of an entrapment zone (E-zone) around the MTOC, in which the microtubule-mediated transport is inhibited. Unlike micro-aggregates, lysosomes scattered in the cytosol are not actively transported into the E-zone, instead they appear to undergo random movement along the microtubule network until they are passively trapped in the E-zone. It may seem puzzling that micro-aggregates and lysosomes use different strategies to get to the E-zone, but one important outcome of this arrangement is that through active transport, micro-aggregates could arrive at the E-zone before lysosomes. As such, the cooperation between p38δ-activated micro-aggregate transport and E-zone-mediated lysosome entrapment ensures the formation of lysosome-clustered aggresomes and directs the orderly disposal of misfolded protein, which is vital to the survival of cells under proteasomal stress.

It is unclear whether the regulatory function of p38δ-SQSTM1 we describe here is important in other autophagy processes. Unlike proteasomal stress-activated autophagy, most autophagy processes, such as starvation-induced autophagy, do not involve active transport of autophagic substrates to the MTOC. Instead, they are first packaged into autophagosomes at the cell periphery before they are transported to the perinuclear region around the MTOC, where most lysosomes are localized (Kast and Dominguez, 2017). Studies have shown that microtubule transport mediated by dynein motors is critical for the targeting of autophagosomes to the MTOC; however, this process does not appear to require p38δ. For example, autophagosomes formed in HeLa cells, where p38δ levels are too low to support aggresome formation, are efficiently transported to the MTOC during serum deprivation (Jahreiss et al., 2008; Kimura et al., 2008). So most likely, p38δ-mediated phosphorylation of SQSTM1 does not have a general regulatory function on microtubule transport during autophagy.

In summary, our study has revealed p38δ-SQSTM1 as a critical signaling module for the recruitment of micro-aggregates to perinuclear aggresomes during proteasomal stress (Fig. S6). This finding has allowed us to further pinpoint suppression of apoptosis as the major cytoprotective mechanism of aggresome formation. Given that aggregation of misfolded proteins has been associated with tissue degeneration and resistance of tumor cells to proteasomal inhibitor drugs, our findings may pave the way to use p38δ as a new therapeutic target for the treatment of different disorders (Abdel Malek et al., 2015; Milan et al., 2015).

MATERIALS AND METHODS

Chemical regents

MG132 and Bafilomycin A_1 (BafA1) were obtained from Merck Millipore (474790, 196000). Bortezomib (Velcade, Bort) was obtained from Selleck Chemicals (S1013).

Plasmid construction

The cDNA clones of human *p38α* (*MAPK14*), *p38β* (*MAPK11*), *p38γ* (*MAPK12*), *p38δ* (*MAPK13*), *CFTR* and *SQSTM1* were obtained from Thermo Fisher Scientific (BC000092, BC027933, BC015741, BC000433, BC156254 and BC003139, respectively). FLAG-tagged HDAC6 expression plasmid and ubiquitin cDNA were obtained from Addgene [plasmid #13823 deposited by Eric Verdin (Fischle et al., 1999) and plasmid #18712 deposited by Edward Yeh (Kamitani et al., 1997), respectively]. Mammalian expression vectors were generated by inserting ORF fragments amplified by PCR from the genes of interest into the corresponding vectors by traditional restriction digestion and ligation, or Gibson assembly (Gibson, 2011). The sequences of the primers used for ORF amplification are listed in Table S1.

Cell culture and transfection

AD293 cell line (Agilent Technologies) and HeLa cell line (American Type Culture Collection), were cultured at 37°C in Dulbecco's modified Eagle's medium (DMEM, Corning, 10-013-CVR) supplemented with 10% fetal bovine serum (FBS, Biowest, S01520), 1% penicillin-streptomycin (Thermo Fisher Scientific, 15140211) in a 5% CO_2 incubator. HEK293FT cell line used for lentivirus production was obtained from Thermo Fisher Scientific, and cells were cultured at 37°C in DMEM supplemented with 10% FBS, 2 mM L-glutamine (Thermo Fisher Scientific, 25030081), 1× non-essential amino acids (NEAAs; Thermo Fisher Scientific, 11140076), 1% penicillin-streptomycin in a 5% CO_2 incubator. Plasmid transfection was carried out with MegaTran 1.0 (OriGene, TT200003). All the cell lines were authenticated and tested for contamination in June, 2017.

Protein extraction

Total protein extract was prepared by homogenizing cells in 1× SDS protein sample buffer and boiling for 5 min. For preparation of soluble and insoluble fractions, cells were lysed in NP40 alternative cell lysis buffer [50 mM Tris-HCl, 150 mM NaCl, pH 8.0, 1 mM EDTA, 1% NP40 Alternative (Merck Millipore, 492016)] on ice for 30 min. The soluble and insoluble fractions were separated by centrifugation at 14,000 ***g*** for 15 min at 4°C. The supernatant of each sample was mixed with 5× SDS sample buffer, and the pellet was solubilized with 1× SDS sample buffer. Both soluble and insoluble samples were boiled for 5 min before SDS-PAGE.

Immunoprecipitation

After treatment, cells were rinsed once with ice-cold PBS and lysed for 30 min on ice in 1% NP40 Alternative cell lysis buffer (as above) containing protease inhibitor cocktail (Thermo Fisher Scientific, 87785) and phosphatase inhibitor cocktail (Thermo Fisher Scientific, 78427). Cell lysates were centrifuged at 14,000 ***g*** for 15 min at 4°C to obtain the soluble fractions. For immunoprecipitiation, 2 µl of primary antibody was added to the soluble fractions for each sample and incubated with rotation at 4°C for 2 h followed by a 1 h incubation with 10 µl Protein-G agarose beads (Merck Millipore, 16-266). The beads were then washed three times with the lysis buffer and resuspended in 1× SDS protein sample buffer. After boiling for 5 min, the samples were analyzed by SDS-PAGE and western blot analysis with indicated antibodies.

Western blot analysis

Protein samples in SDS sample buffer were separated by SDS-PAGE and transferred to Immunobilon-FL PVDF membrane (Merck Millipore, IPFL00010). After blocking with 5% non-fat dry milk in TBST (TBS, pH 7.4, 0.2% Tween-20), the membrane was incubated with primary antibodies at 4°C overnight. The membrane was then washed three times with TBST and incubated with Dylight 680 and/or Dylight 800-conjugated secondary antibodies (KPL) in the dark for 2 h. After three washes with TBST, the image was acquired by Li-Cor Odyssey Clx Infrared Imaging System (LI-COR Biotechnology, Lincoln, NE, USA). Primary antibodies against the following proteins were used for western blot analysis: SQSTM1 (Proteintech, 18420-1-AP), Phospho-SQSTM1(Thr269/Ser272; Phosphosolutions, P196-269), K48-linked Ub chain-specific antibody (Merck Millipore, 05-1307), p38α (R&D Systems, AF8691), p38β (Cell Signaling Technology, 2339), p38γ (R&D Systems, AF1347), p38δ (R&D Systems, AF1519), Phospho-p38 (Thr180/Tyr182; Cell Signaling Technology, 4511), TRAF6 (Cell Signaling Technology, 8028), MEKK3 (Cell Signaling Technology, 5727), ATG5 (Cell Signaling Technology, 12994), FLAG Tag (Prospec, ANT-146-b), MYC tag (BioLegend, MMS-150R), GAPDH (Zen Bioscience, 200306), β-tubulin (Zen Bioscience, 200608) and β-actin (Zen Bioscience, 200068-6D7). See Table S3 for further details and dilutions of all antibodies.

Immunostaining and image analysis

Immunostaining was performed essentially as described previously. In brief, cells were fixed with 4% paraformaldehyde in PBS for 15 min, permeabilized with 0.2% Triton X-100 (Merck Millipore, 9410-1L) in PBS for 15 min, and then blocked with 5% goat serum (Jackson ImmunoResearch Laboratories, 005-000-12) for 1 h. The slides were incubated with primary antibodies at room temperature for 2 h followed by an incubation for 1 h with Alexa Flour 488- or 568-conjugated secondary antibodies (Thermo Fisher Scientific, A11034, A11029, A11031, A11036) in the dark. After staining the nuclei with DAPI solution (Merck Millipore, 508741) for 5 min, the slides were mounted for fluorescence microscopy. Images were obtained with Olympus FV1000 confocal microscope (Olympus, Tokyo, Japan). The following primary antibodies were used for immunostaining: SQSTM1 (Proteintech, 18420-1-AP), FLAG Tag (Propec, ant-146-b), K48-linked Ub chain-specific antibody (Merck Millipore, 05-1307) and p38δ (R&D Systems, AF1519). See Table S3 for further details and dilutions of all antibodies.

Generation of knockout cell lines

The SQSTM1$^{-/-}$ cell line was generated with the TALEN system as described earlier (Gao et al., 2016). The p38α, p38β, p38γ, p38δ, MEKK3, TRAF6 and ATG5 knockout cell lines were generated from AD293 cells using a CRISPR/Cas9 system (Cong et al., 2013; Mali et al., 2013). Briefly, two gRNA expression plasmids were transfected into AD293 cells with Cas9 expression vector. After 24 h, cells were diluted and seeded in 96-well plates to form single colonies. The clones were expanded and analyzed by western blot analysis and genomic PCR to isolate knockout cell lines. The guide sequences and their genomic localization for human p38α, p38β, p38γ, p38δ, MEKK3, TRAF6 and ATG5 genes are listed in Table S2.

Generation of stable expression cell lines

The DNA fragments corresponding to the ORFs of p38γ(WT)-FLAG, p38δ(WT)-FLAG, FLAG-SQSTM1(WT), FLAG-SQSTM1(T269A/S272A) and FLAG-SQSTM1(T269E/S272D) were transferred into pLVX-puro lentiviral vector (Clontech, 632164), then transfected into HEK293FT cells with lentiviral helper plasmids: pLP1, pLP2 and pLP/VSVG (Thermo Fisher Scientific, K497500). The virus-containing cell culture medium was harvested 40 h later and used to transduce cell lines indicated. After 48 h, the transduced cells were selected by growing in the DMEM growth medium containing 0.5 µg/ml puromycin (InvivoGen, ant-pr-5), and expression of the rescue gene was verified by western blot analysis and immunofluorescence staining.

Cell death assay

Cell death assay was performed with CF488A-Annexin V (ANXA5) and propidium iodide (PI) apoptosis Kit (Biotium, 30061) as described previously. Briefly, cells grown on 10 cm dishes were treated with DMSO or 2 µM MG132 for 18 h, then harvested by digestion with 0.05% trypsin-EDTA solution. The cells were washed twice with PBS and resuspended in 100 µl ANXA5 Binding Buffer. They were then incubated with 15 µl CF488A-ANXA5 and 5 µl PI in the dark for 15 min at room temperature. The cells were next washed twice with the binding buffer, and mounted onto slides. Images were acquired with a Nikon Eclipse 80i fluorescence microscope equipped with Nikon PLAN FLUOR 40× objective.

Statistics

Each experiment was performed at least three times. Fluorescence images from aggresome formation and cell death assay results were quantified manually. Data are presented as mean±s.e.m. Within each group, statistical significance was determined by using the Student's *t*-test.

Competing interests
The authors declare no competing or financial interests.

Author contributions
Conceptualization: J.G., C.J.; Methodology: C.Z., J.G.; Investigation: C.Z., M.L., Y.D.; Data curation: C.Z.; Writing - original draft: C.Z.; Supervision: C.J.; Project administration: C.Z.; Funding acquisition: C.J.

Funding
This work was supported by research grants from the Ministry of Science and Technology of China (973 Basic Research Program grant 2009CB941404 to C.J.), the National Natural Science Foundation of China (grant 30871032 to C.J.) and Department of Science and Technology of Sichuan Province (Young Scientific Innovation Team in Neurological Disorders grant 2011JTD0005 to C.J. and grant 2016FZ0109 to C.J.).

Supplementary information
Supplementary information available online at
http://jcs.biologists.org/lookup/doi/10.1242/jcs.216671.supplemental

References
Abdel Malek, M. A., Jagannathan, S., Malek, E., Sayed, D. M., Elgammal, S. A., Abd El-Azeem, H. G., Thabet, N. M. and Driscoll, J. J. (2015). Molecular chaperone GRP78 enhances aggresome delivery to autophagosomes to promote drug resistance in multiple myeloma. *Oncotarget* **6**, 3098-3110.

Askari, N., Diskin, R., Avitzour, M., Capone, R., Livnah, O. and Engelberg, D. (2007). Hyperactive variants of p38alpha induce, whereas hyperactive variants of p38gamma suppress, activating protein 1-mediated transcription. *J. Biol. Chem.* **282**, 91-99.

Bjørkøy, G., Lamark, T., Brech, A., Outzen, H., Perander, M., Øvervatn, A., Stenmark, H. and Johansen, T. (2005). p62/SQSTM1 forms protein aggregates degraded by autophagy and has a protective effect on huntingtin-induced cell death. *J. Cell Biol.* **171**, 603-614.

Cong, L., Ran, F. A., Cox, D., Lin, S., Barretto, R., Habib, N., Hsu, P. D., Wu, X., Jiang, W., Marraffini, L. A. et al. (2013). Multiplex genome engineering using CRISPR/Cas systems. *Science* **339**, 819-823.

Coulthard, L. R., White, D. E., Jones, D. L., McDermott, M. F. and Burchill, S. A. (2009). p38(MAPK): stress responses from molecular mechanisms to therapeutics. *Trends Mol. Med.* **15**, 369-379.

Cuadrado, A. and Nebreda, A. R. (2010). Mechanisms and functions of p38 MAPK signalling. *Biochem. J.* **429**, 403-417.

Durán, A., Serrano, M., Leitges, M., Flores, J. M., Picard, S., Brown, J. P., Moscat, J. and Diaz-Meco, M. T. (2004). The atypical PKC-interacting protein p62 is an important mediator of RANK-activated osteoclastogenesis. *Dev. Cell* **6**, 303-309.

Fischle, W., Emiliani, S., Hendzel, M. J., Nagase, T., Nomura, N., Voelter, W. and Verdin, E. (1999). A new family of human histone deacetylases related to Saccharomyces cerevisiae HDA1p. *J. Biol. Chem.* **274**, 11713-11720.

Fortun, J., Dunn, W. A., Jr, Joy, S., Li, J. and Notterpek, L. (2003). Emerging role for autophagy in the removal of aggresomes in Schwann cells. *J. Neurosci.* **23**, 10672-10680.

Gao, J., Li, M., Qin, S., Zhang, T., Jiang, S., Hu, Y., Deng, Y., Zhang, C., You, D., Li, H. et al. (2016). Cytosolic PINK1 promotes the targeting of ubiquitinated proteins to the aggresome-autophagy pathway during proteasomal stress. *Autophagy* **12**, 632-647.

Gibson, D. G. (2011). Enzymatic assembly of overlapping DNA fragments. *Methods Enzymol.* **498**, 349-361.

Hamdan, N., Kritsiligkou, P. and Grant, C. M. (2017). ER stress causes widespread protein aggregation and prion formation. *J. Cell Biol.* **216**, 2295-2304.

Jahreiss, L., Menzies, F. M. and Rubinsztein, D. C. (2008). The itinerary of autophagosomes: from peripheral formation to kiss-and-run fusion with lysosomes. *Traffic* **9**, 574-587.

Johnston, J. A., Ward, C. L. and Kopito, R. R. (1998). Aggresomes: a cellular response to misfolded proteins. *J. Cell Biol.* **143**, 1883-1898.

Kamitani, T., Kito, K., Nguyen, H. P. and Yeh, E. T.(1997). Characterization of NEDD8, a developmentally down-regulated ubiquitin-like protein. *J. Biol. Chem.* **272**, 28557-8562.

Kast, D. J. and Dominguez, R. (2017). The cytoskeleton-autophagy connection. *Curr. Biol.* **27**, R318-R326.

Kawaguchi, Y., Kovacs, J. J., McLaurin, A., Vance, J. M., Ito, A. and Yao, T.-P. (2003). The deacetylase HDAC6 regulates aggresome formation and cell viability in response to misfolded protein stress. *Cell* **115**, 727-738.

Kawai, K., Saito, A., Sudo, T. and Osada, H. (2008). Specific regulation of cytokine-dependent p38 MAP kinase activation by p62/SQSTM1. *J. Biochem.* **143**, 765-772.

Kimura, S., Noda, T. and Yoshimori, T. (2008). Dynein-dependent movement of autophagosomes mediates efficient encounters with lysosomes. *Cell Struct. Funct.* **33**, 109-122.

Koul, H. K., Pal, M. and Koul, S. (2013). Role of p38 MAP kinase signal transduction in solid tumors. *Genes Cancer* **4**, 342-359.

Lim, J., Lachenmayer, M. L., Wu, S., Liu, W., Kundu, M., Wang, R., Komatsu, M., Oh, Y. J., Zhao, Y. and Yue, Z. (2015). Proteotoxic stress induces phosphorylation of p62/SQSTM1 by ULK1 to regulate selective autophagic clearance of protein aggregates. *PLoS Genet.* **11**, e1004987.

Lin, X., Li, S., Zhao, Y., Ma, X., Zhang, K., He, X. and Wang, Z. (2013). Interaction domains of p62: a bridge between p62 and selective autophagy. *DNA Cell Biol.* **32**, 220-227.

Linares, J. F., Duran, A., Yajima, T., Pasparakis, M., Moscat, J. and Diaz-Meco, M. T. (2013). K63 polyubiquitination and activation of mTOR by the p62-TRAF6 complex in nutrient-activated cells. *Mol. Cell* **51**, 283-296.

Mali, P., Yang, L., Esvelt, K. M., Aach, J., Guell, M., DiCarlo, J. E., Norville, J. E. and Church, G. M. (2013). RNA-guided human genome engineering via Cas9. *Science* **339**, 823-826.

Matsumoto, G., Wada, K., Okuno, M., Kurosawa, M. and Nukina, N. (2011). Serine 403 phosphorylation of p62/SQSTM1 regulates selective autophagic clearance of ubiquitinated proteins. *Mol. Cell* **44**, 279-289.

Milan, E., Perini, T., Resnati, M., Orfanelli, U., Oliva, L., Raimondi, A., Cascio, P., Bachi, A., Marcatti, M., Ciceri, F. et al. (2015). A plastic SQSTM1/p62-dependent autophagic reserve maintains proteostasis and determines proteasome inhibitor susceptibility in multiple myeloma cells. *Autophagy* **11**, 1161-1178.

Mizushima, N. (2007). Autophagy: process and function. *Genes Dev.* **21**, 2861-2873.

Ouyang, H., Ali, Y. O., Ravichandran, M., Dong, A., Qiu, W., MacKenzie, F., Dhe-Paganon, S., Arrowsmith, C. H. and Zhai, R. G. (2012). Protein aggregates are recruited to aggresome by histone deacetylase 6 via unanchored ubiquitin C termini. *J. Biol. Chem.* **287**, 2317-2327.

Park, S., Ha, S.-D., Coleman, M., Meshkibaf, S. and Kim, S. O. (2013). p62/SQSTM1 enhances NOD2-mediated signaling and cytokine production through stabilizing NOD2 oligomerization. *PLoS ONE* **8**, e57138.

Sha, Y., Pandit, L., Zeng, S. and Eissa, N. T. (2009). A critical role for CHIP in the aggresome pathway. *Mol. Cell. Biol.* **29**, 116-128.

Szeto, J., Kaniuk, N. A., Canadien, V., Nisman, R., Mizushima, N., Yoshimori, T., Bazett-Jones, D. P. and Brumell, J. H. (2006). ALIS are stress-induced protein storage compartments for substrates of the proteasome and autophagy. *Autophagy* **2**, 189-199.

Tamás, M. J., Sharma, S. K., Ibstedt, S., Jacobson, T. and Christen, P. (2014). Heavy metals and metalloids as a cause for protein misfolding and aggregation. *Biomol.* **4**, 252-267.

Travassos, L. H., Vasconcellos, L. R. C., Bozza, M. T. and Carneiro, L. A. M. (2017). Heme and iron induce protein aggregation. *Autophagy* **13**, 625-626.

Zaarur, N., Meriin, A. B., Bejarano, E., Xu, X., Gabai, V. L., Cuervo, A. M. and Sherman, M. Y. (2014). Proteasome failure promotes positioning of lysosomes around the aggresome via local block of microtubule-dependent transport. *Mol. Cell. Biol.* **34**, 1336-1348.

Zatloukal, K., Stumptner, C., Fuchsbichler, A., Heid, H., Schnoelzer, M., Kenner, L., Kleinert, R., Prinz, M., Aguzzi, A. and Denk, H. (2002). p62 Is a common component of cytoplasmic inclusions in protein aggregation diseases. *Am. J. Pathol.* **160**, 255-263.